THE JOURNAL OF PHYSICAL CHEMISTRY A

Article

pubs.acs.org/JPCA

Tunneling Lifetime of the *ttc*/VIp Conformer of Glycine in Low-Temperature Matrices

Gábor Bazsó, Gábor Magyarfalvi, and György Tarczay*

Laboratory of Molecular Spectroscopy, Institute of Chemistry, Eötvös University, P.O. Box 32, H-1518, Budapest 112, Hungary

Supporting Information

ABSTRACT: Conformer ***ttc*/VIp** of glycine and glycine-N,N,O-d_3 has been prepared in low-temperature Ar, Kr, Xe, and N_2 matrices by near-infrared (NIR) laser irradiation of the first OH stretching overtone of conformer ***ttt*/Ip**. Glycine (and glycine-N,N,O-d_3) ***ttc*/VIp** was found to convert back to ***ttt*/Ip** in the dark by hydrogen-atom tunneling. The observed half-lives of ***ttc*/VIp** in Ar, Kr, and Xe matrices at 12 K were 4.4 ± 1 s (50.0 ± 1 h), 4.0 ± 1 s (48.0 ± 1 h), and 2.8 ± 1 s (99.3 ± 2 h), respectively. In correspondence with the observation for the *cis*-to-*trans* conversion of formic and acetic acid, the tunneling half-life of glycine ***ttc*/VIp** in a N_2 matrix is more than 3 orders of magnitude longer (6.69×10^3 and 1.38×10^4 s for two different sites) than in noble gas matrices due to complex formation with the host molecules. The present results are important to understand the lack of experimental observation of some computationally predicted conformers of glycine and other amino acids.

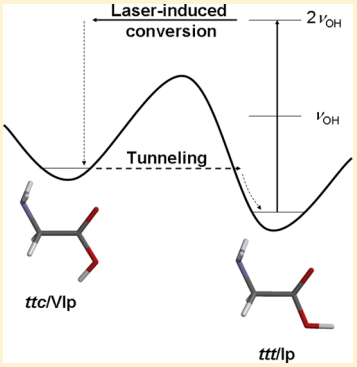

1. INTRODUCTION

The tunneling mechanism is a very important phenomenon both in physical chemistry and biochemistry that can be best studied at low temperatures, where the classical reaction pathways are thermally unavailable. One of the most suitable experimental methods to study conformational conversions by hydrogen-atom tunneling is matrix isolation (MI) spectroscopy. Although hydrogen-atom tunneling in many small organic molecules has been studied by this method,[1−39] very few recent works investigated biomolecules; these included cytosine,[40] NADH mimicking model compounds,[41] and in a preliminary study by our group, glycine.[42] It is, however, now widely accepted in biochemistry that enzyme-catalyzed hydrogen-transfer reactions cannot be fully understood and modeled without taking into account quantum tunneling effects.[43,44] MI studies can thus add valuable information of understanding tunneling in biomolecules and probably in even larger biochemical systems. Glycine, whose conformational distribution and dynamics have extensively been studied both by experimental[42,45−62] and theoretical methods,[63−83] is an attractive target for study.

The most accurate computed relative energies[62,68] with thermal corrections[78] for glycine agree that at least four conformers should be present in detectable amounts in the gas-phase. In the 358−438 K temperature range, these are, using the labeling of both Balabin and Császár,[62,68] ***ttt*/Ip**, ***ccc*/IIn**, ***gtt*/IVn**, and ***tct*/IIIp** (see Figure 1). In contrast to the theoretical predictions, only the ***ccc*/IIn** and the ***ttt*/Ip** conformers were identified by microwave (MW) spectroscopic studies.[45−52] The first matrix-isolation IR (MI-IR) studies also identified these two conformers only.[53,54] Later MI-IR studies showed that the ***tct*/IIIp** conformer can also be trapped in the matrix if the sample is deposited at lower temperatures below

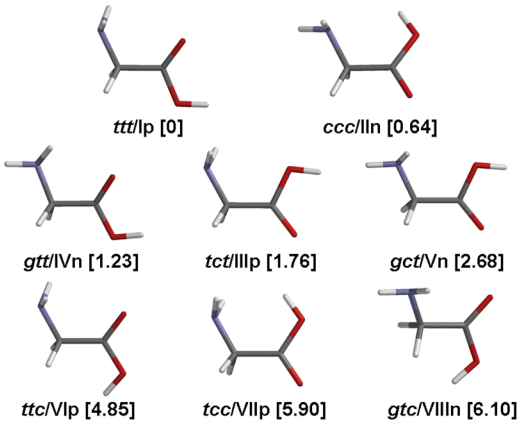

Figure 1. Conformers of glycine. In the square brackets, the relative energies are given in kcal mol^{-1} as computed using the focal-point analysis by Balabin.

13 K,[55−61] and this conformer can be converted to the ***ttt*/Ip** conformer by annealing the Ar matrix at 20−35 K.[55,61] The same three conformers were observed in the IR spectrum of glycine in He droplets.[59] In none of these studies was the fourth low-energy conformer, ***gtt*/IVn**, identified. Recently Balabin has reported the identification of conformer ***gtt*/IVn** by jet-cooled Raman spectroscopy at short distances from the nozzle.[62] Increasing the distance between the observation point and the nozzle outlet, the intensity of the bands assigned to ***gtt*/IVn** dropped rapidly.

Received: August 2, 2012
Revised: September 14, 2012
Published: October 12, 2012

   dx.doi.org/10.1021/jp3076436 | J. Phys. Chem. A 2012, 116, 10539−10547

The absence of the ***gtt*/IVn** and the ***tct*/IIIp** conformers under jet-cooled MW conditions was explained as a consequence of conformational cooling to the ***ttt*/Ip** form via low-energy interconversion barriers in the free jet expansion and by the small dipole moment of ***tct*/IIIp**.[84] In order to understand the cause of the missing conformers in the MW, MI-IR, and He droplet measurements, Miller et al. have investigated the interconversion barriers and the collision-induced conformational change in glycine using quantum dynamical calculations.[78,85] According to their computations, the ***gtt*/IVn** → ***ttt*/Ip** and the ***tct*/IIIp** → ***ttt*/Ip** barrier heights are almost equal, and they have found that under jet expansion conditions the ***gtt*/IVn** → ***ttt*/Ip** conversion process involves both classical and hydrogen tunneling effects, while in the ***tct*/IIIp** → ***ttt*/Ip** conversion only classical effects contribute. Nevertheless, according to their simulations for jet expansion conditions (for 100 K), the calculations presented little indication that the ***gtt*/IVn** → ***ttt*/Ip** conversion occurs more readily than the ***tct*/IIIp** → ***ttt*/Ip** conversion process. These inconclusive theoretical and experimental results clearly show that further experimental data and theoretical simulations are needed in order to understand the tunneling processes in glycine.

The purpose of the present study is to determine the experimental tunneling lifetime of another conformer, ***ttc*/VIp**. In a recent paper, we reported the preparation of this previously experimentally unobserved conformer by laser irradiation of the first OH stretching overtone of conformer ***ttt*/Ip**,[42] and we have also shown that ***ttc*/VIp** decays in the dark. A preliminary half-life value of 5 ± 2 s in an Ar matrix at ∼12 K was reported. With the present report we considerably extend this former study by measuring the accurate lifetimes of the ***ttc*/VIp** conformer of both glycine and its deuterated isotopologue, glycine-N,N,O-d_3. In order to study the effect of the host, the lifetimes were determined in four different matrices: in Ar, Kr, Xe, and N_2. It is expected that not only the substitution of hydrogen by deuterium, but, based on former studies on formic and acetic acids,[12,14] also the use of N_2 matrix instead of Ar lengthens the lifetime of this short-lived conformer. The extended lifetime allows the experimental observations of weaker spectral features, which could not be observed in Ar matrix. As part of the conclusions of the present study, we briefly discuss the possibility of the preparation and identification of other short-lived conformers of glycine.

2. METHODS

2.1. MI-IR Measurements. Glycine (Reanal, purity >99%) and glycine-N,N,O-d_3 (Aldrich, purity >98%) were evaporated into a vacuum chamber using a home-built Knudsen effusion cell. The evaporated sample was mixed with argon (Messer, 99.9997%), krypton (Messer, 99.998%), xenon (Messer, 99.998%), or nitrogen (Messer, 99.999%) before deposition. The gas flow was kept at ∼0.07 mmol min^{-1}, and the evaporation temperature was ∼407 ± 5 K. The sample−rare gas mixture was deposited onto a cold (8−10 K for mid-infrared (MIR), 12−14 K for near-infrared (NIR)) CsI window, mounted on a Janis CCS-350R cold head cooled by a CTI Cryogenics 22 closed-cycle refrigerator unit. The temperature of the cold window was controlled by a Lake Shore 321 thermostat equipped with a silicon diode thermometer. The cold window was set at 45° to the optical path of the spectrometer, and the irradiating laser beam was perpendicular to the optical path.

All the MI-IR spectra were recorded on a Bruker IFS 55 spectrometer using a mercury cadmium telluride (MCT) detector with a tungsten lamp for the 2500−8000 cm^{-1} (NIR) and with a Globar source for the 600−4000 cm^{-1} (MIR) spectral region. The spectra were recorded at 1 cm^{-1} instrumental resolution. For the measurement of overtones in the NIR region, at least 1000 scans were accumulated, while in the MIR spectral region spectra consisted of at least 50 scans.

Conformational changes were selectively induced by an optical parametric oscillator (VersaScan MB 240 OPO, GWU/Spectra Physics) pumped with the third harmonic (355 nm) of a pulsed (10 Hz, 2−3 ns) Quanta Ray Lab 150 Nd:YAG laser (Spectra Physics). The line width of the idler (NIR) output of the OPO was about 5 cm^{-1}, and pulse energies were 10−15 mJ in the OH first overtone region and 8−11 mJ in the OD first overtone region. The laser beam was unfocused; its diameter was of about 0.8 cm. The OPO was calibrated in former experiments by optimizing for the shortest bleaching time of an irradiated species monitored by FT-IR measurements.

In the case of lifetimes shorter than a few minutes (glycine in Ar, Kr, and Xe matrices), scans as short as possible were recorded, i.e., single scans were recorded with a repetition rate of 3.8 s. The laser radiation was switched on at the beginning of a 20 scan cycle, and it was switched off after the 10th scan, i.e., the 11−20th scan was recorded in the dark. This cycle was repeated 16 times, and the corresponding scans from each cycle were averaged. In these cases, the spectra were obtained as the average of 16 acquisitions. In order to record the spectra during the laser irradiation, an LPW 3860 low pass filter was placed between the cold window and the detector.

In the case of lifetimes on the order of a few hours (glycine in N_2 matrix), 50 scans were recorded every 5 min. In order to prevent the conformational conversion caused by the excitation of the overtone modes by the Globar source, the LPW 3860 low pass filter was placed between the source and the cold window.

For lifetimes on the scale of days (glycine-d_3) 64−250 scans (4−15 min) were accumulated in an average of every 8 h. During the measurements, the LPW 3860 low pass filter was between the source and the cold window, and the source was completely blocked between the measurements.

2.2. Computational Details. Quantum chemical calculations were performed by the PQS (Parallel Quantum Solutions) 3.2[86] and by the Gaussian 09[87] program packages. Initial geometries for geometry optimizations were roughly set to the previously reported structures, and were optimized at the B3LYP[88]/6-31++G**[89] and MP2[90]/6-311++G**[91] levels of theory. The optimizations were followed by second derivative calculations to determine whether the obtained stationary points correspond to minima. The barrier heights between the conformers were computed also at the B3LYP/6-31++G**[91d] and the MP2/6-311++G** levels of theory.

Harmonic vibrational frequencies and intensities were calculated at the B3LYP/6-31++G** level of theory using the scaled quantum mechanical (SQM) force field scheme[92,93] with scaling factors determined by Fábri et al.[94]

Tunneling rates were estimated at the MP2/6-311++G** level of theory by the help of the Multiwell program package, which applies the Eckart model for tunneling through an unsymmetrical barrier.[96]

3. RESULTS AND DISCUSSION

3.1. NIR Irradiation Induced Conformational Conversion and Spectral Assignments. Figure 2 presents the first OH and NH stretching overtone region of the MI-NIR spectra of glycine and glycine-d_3 recorded in Ar, Kr, Xe, and N_2 matrices. On the basis of the previously published MI studies on glycine, all the dominant transitions can be assigned to conformers ***ttt*/Ip** and ***ccc*/IIn**. Conformer ***tct*/IIIp** is present only in traces, since it converts to conformer ***ttt*/Ip** when it is deposited at >14 K. The observed vibrational wavenumbers of the overtones are collected in Table 1.

Table 1. First Overtones of the O(H/D) and N(H/D) Stretching Modes (in cm^{-1}) of Glycine and Glycine-d_3 Conformers in Ar, Kr, Xe, and N_2 Matrices[a]

	glycine	glycine-d_3
	***ttt*/Ip** $2\nu_{O(H/D)}$	
Ar	6961, 6965, 6958, 6957, 6946	5175, 5167, 5160
Kr	6944, 6935, 6931, 6924	5159, 5150, 5144
Xe	6931, 6906, 6896	5150, 5136, 5127
N_2	6933, 6922	5148, 5140
	***ttt*/Ip** $2\nu_{N(H/D)}$	
Ar	6615, 6606, 6573	5077, 5067, 5060, 5048
Kr	6593, 6562	5066, 5036
Xe	6573, 6537	5058, 5031
N_2	6624, 6586	5063
	***ccc*/IIn** $2\nu_{O(H/D)}$	
Ar	5059, 5052	
Kr	5040[b]	
Xe	5035[b]	
N_2		
	***ccc*/IIn** $2\nu_{N(H/D)}$	
Ar	6669, 6657	5092[b]
Kr	6635[b]	5081[b]
Xe	6620[b]	5074[b]
N_2	6680[b]	

[a]In each case, multiple lines were observed due to site splitting. In the case of glycine-d_3, some of the less intensive peaks (e.g., at 4900, 4837 (in Ar), 4890, 4830 (in Kr), 4874, 4813 (in Xe) and at 4899 and 4839 cm^{-1} (in N_2)) likely belong to combination bands or to vibrational transitions of glycine-d_2 species. When the matrix is deposited below 12−14 K, or after NIR laser irradiation, traces of the conformer ***tct*/IIIp** can also be identified in the NIR spectrum (see ref 42). [b]Tentative assignments.

The MI-MIR spectra of glycine and glycine-d_3 together with difference spectra are shown in Figures 3 and 4. The latter were obtained by subtracting the spectra measured after deposition from the spectra recorded after irradiating the first OH stretching overtone (see the wavenumber of the irradiating laser in Figure 2) of conformer ***ttt*/Ip** in the most abundant site. (In the case of Xe matrix, the first OH stretching overtone of conformer ***ttt*/Ip** in two different sites were irradiated. These two irradiation experiments led to the increase of the same peaks.) In every NIR irradiation experiment, the formation of ***ttc*/VIp** (see, e.g., the characteristic bands on the higher wavenumber side of both the O−H/D and the C=O stretching band of ***ttt*/Ip**) at the expense of ***ttt*/Ip** was observed. In addition to this, other conversion processes were also found. These are discussed in detail for glycine in Ar and Kr matrices in ref 42. Briefly, the amount of ***ttt*/Ip** in the site(s) not irradiated and also the amount of conformer ***tct*/IIIp**

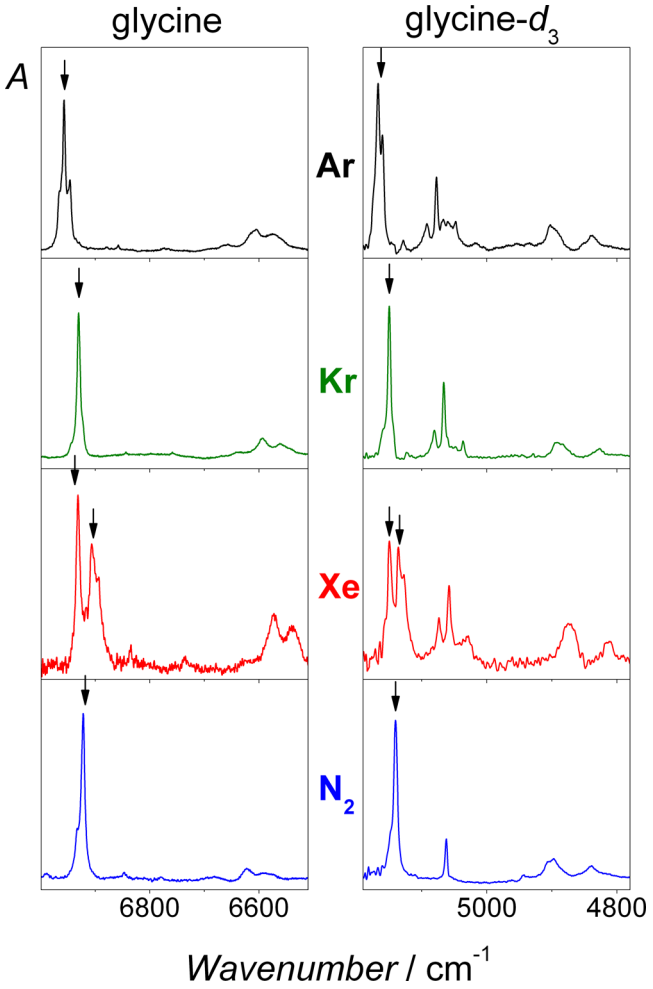

Figure 2. MI-NIR spectra of glycine and glycine-d_3 in Ar, Kr, Xe, and N_2 matrices. (The red-shifted first OH stretching overtone of conformer ***ccc*/IIn** is outside of the displayed region.) The arrows show the positions where the laser was tuned to produce the ***ttc*/VIp** conformer.

changed during the irradiation in Ar, Kr, and Xe matrices. The concentration of ***tct*/IIIp** increased at the expense of ***ttt*/Ip** when the laser was set to the higher wavenumber side of the OH stretching overtone band of conformer ***ttt*/Ip**. This concentration decreased when the laser was set to the lower wavenumber side of the OH stretching overtone band of conformer ***ttt*/Ip** because of an overlap of the laser line with the O(H/D) stretching overtone of ***tct*/IIIp**.

The ***ttt*/Ip** → ***ttc*/VIp** conversion induced by NIR irradiation is most efficient for glycine in a N_2 matrix: approximately 50−60% conversion could be reached in about 30−40 min. Due to the fast back conversion (see next section) of ***ttc*/VIp** to ***ttt*/Ip**, the steady-state ratio of ***ttc*/VIp** and ***ttt*/Ip** (estimated to be ∼0.5%) is reached in Ar, Kr, and Xe matrices in about 20−30 s (see Figure 5). Assuming that the concentration is approximately 1:1000, the isomerization quantum yield can be estimated by the approach of refs 6, 9, and 17. The quantum yields received for Ar, Kr, and Xe matrices are 8×10^{-4}, 1×10^{-3}, and 2×10^{-3}, respectively. These values are roughly 1 and 2 orders of magnitude smaller than the quantum yield measured for the *trans*→*cis* isomerization of propionic (1.4×10^{-2}) and formic acid (1.7×10^{-1}) when their first OH stretching overtone is irradiated in an Ar matrix.[9]

dx.doi.org/10.1021/jp3076436 | J. Phys. Chem. A 2012, 116, 10539−10547

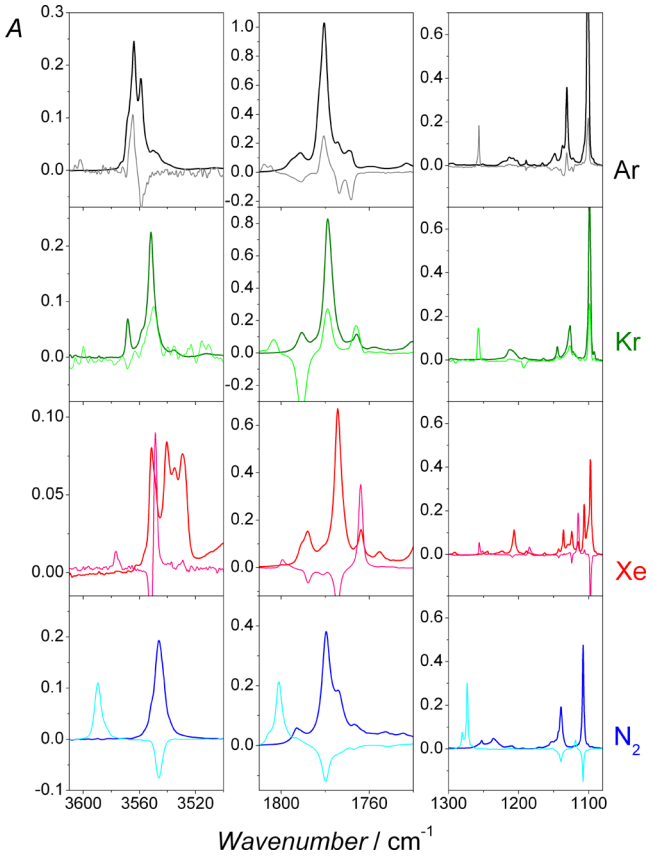

Figure 3. Fundamental O−H stretching, C═O stretching, and C−O−H bending/C−O stretching regions from the MI-IR spectra of glycine in Ar (black), Kr (green), Xe (red), and N_2 (blue) matrices (thick, dark lines), and the difference of spectra recorded after and before NIR laser irradiation (~0.5 min for Ar, Kr and Xe, and ~40 min for N_2 matrix) at the first overtone of O−H stretching (at 6946 cm^{-1} in Ar, 6931 cm^{-1} in Kr and Xe, and 6922 cm^{-1} in N_2 matrix) of conformer ***ttt*/Ip** (thin, light lines; multiplied by 100 for Ar, Kr, and Xe matrices).

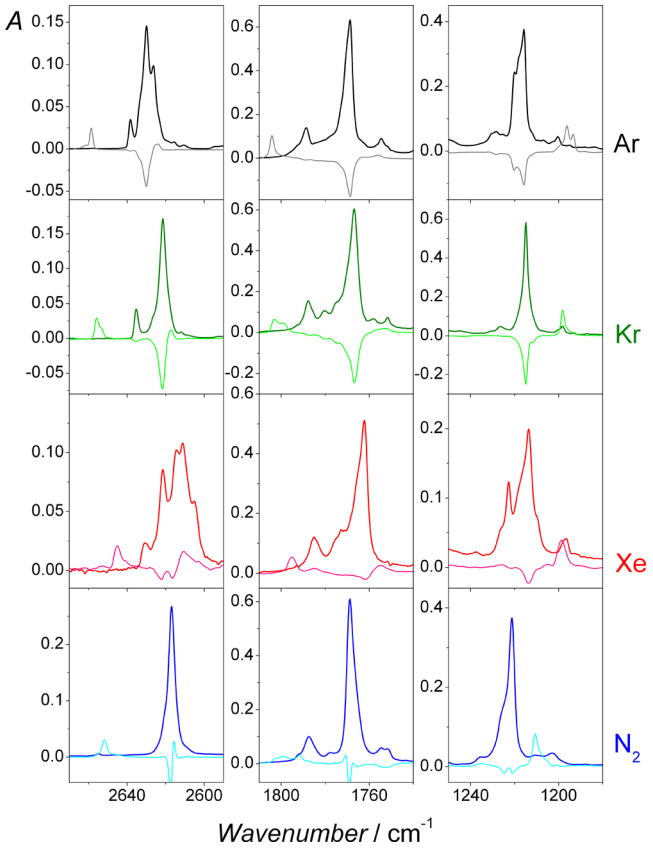

Figure 4. Fundamental O−D, C═O stretching, and C−O−D bending regions from the MI-IR spectra of glycine-d_3 in Ar (black), Kr (green), Xe (red), and N_2 (blue) matrices (thick, dark lines), and the difference of spectra recorded after and before 1.5−2.5 h NIR laser irradiation at the first overtone of O−D stretching (at 5167 cm^{-1} in Ar, 5150 cm^{-1} in Kr and Xe, and 5140 cm^{-1} in N_2 matrix) of conformer ***ttt*/Ip** (thin, light lines).

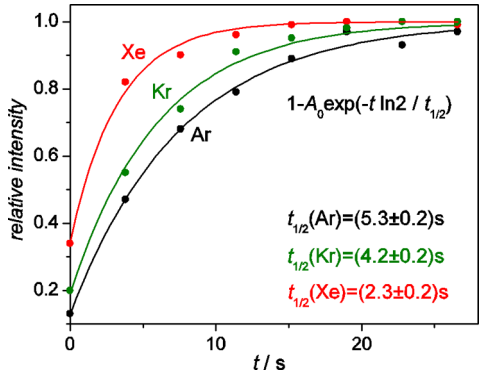

Figure 5. Change of the relative intensities of the bands of glycine conformer ***ttc*/VIp** during NIR laser irradiation.

In the case of glycine-d_3, the conversion was somewhat slower in each matrix; 5−20% of ***ttt*/Ip** can be converted to ***ttc*/VIp** in about 2 h. The slower conversion rate can be explained by the somewhat lower intensity of the irradiation laser light in the OD than in the OH stretching region. In addition to this, the different couplings of the O(H/D) stretching to other vibrational modes, and the fact that the first overtone of the OD stretching vibrational energy level is close to the ***ttc*/VIp** to ***ttt*/Ip** barrier (the zero-point vibrational energy corrected MP2/6-311++G** barrier height is 4042 cm^{-1}) can also be responsible for the less effective conversion. (The corresponding OH stretching vibrational level is well above this barrier.)

Because of the low steady-state ratio between the ***ttc*/VIp** and ***ttt*/Ip** conformers in the Ar, Kr, and Xe matrices, other conformers, especially the ***tct*/IIIp** conformer, also appear in those three difference spectra, making them more complicated than the difference spectra recorded in N_2 or for glycine-d_3 (see Figures 3 and 4).

Based on the different conversion rates upon NIR irradiation, the spectral bands can unambiguously be assigned to conformers ***ttt*/Ip**, ***ccc*/IIn**, ***tct*/IIIp**, and ***ttc*/VIp**. The assignment of the bands of ***ttc*/VIp** is further supported by their decay in the dark (see next section). The different decay rates clearly distinguish two different sites in the N_2 matrix. Tables 2 and 3 summarize the assignments of the MI-MIR spectra of the ***ttc*/VIp** conformer of glycine and glycine-d_3 in Ar, Kr, Xe, and N_2. The spectral assignments of the other three conformers are given in the Supporting Information and (for glycine in Ar and Kr matrices) in ref 42.

3.2. Tunneling Rates. The dark process taking place after the irradiation of the first OH stretching overtone of conformer ***ttt*/Ip** is demonstrated in Figure 6 by the selected regions of the IR spectra of glycine in Ar and N_2 matrices, and glycine-d_3 in an Ar matrix. These spectra reveal that ***ttc*/VIp** converts back to ***ttt*/Ip** with very different half-lives for glycine and glycine-d_3.

dx.doi.org/10.1021/jp3076436 | J. Phys. Chem. A 2012, 116, 10539−10547

Table 2. Computed (SQM B3LYP) Fundamental Frequencies ($\tilde{\nu}$ in cm^{-1}), Intensities (I in km mol^{-1}) and Experimental Vibrational Transitions ($\tilde{\nu}$ in cm^{-1}) of the *ttc*/VIp Conformer of Glycine

					N_2 matrix	
$\tilde{\nu}$	I	Ar matrix	Kr matrix	Xe matrix	site A	site B
3604	42	3602.1w, 3606.1w	3600.1vw	3576.8w	3590.4w	3588.9w
3425	8				3447.3vw, 3409.9vw	3445.8vw, 3411.3vw
3348	3					
2937	12				2956.5vw	2952.0vw
2899	28				2912.7vw	2921.0vw
1795	256	1804.7s, 1807.7s	1803.4s	1799.7m	1801.1s, 1895.8w	1805.0s, 1794.0w
1642	29				1652.8w	1650.8w
1434	8				1430.1w, 1403.5w	1430.1w, 1403.5w
1365	0				1369.7w	1369.7w
1352	20				1343.4w	1349.8w
1253	376	1256.6vs, 1259.3s	1257.4vs	1256.3s	1273.5vs, 1266.7vs	1280.7vs
1156	0					
1132	5					
1092	44	1109w (or 1101w)[a]	1109.5w		1119.1w	1118.8w
906	1				919.2	919.2
884	180	883.8m[a]	884.3m	881.3m	888.4m	889.6m
805	33			808.1m	821.5m	816.8m
643	16					
558	14					
459	2					
435	95					
259	30					
216	72					
72	7					

[a]Uncertain assignment due to nearby bands of other conformers.

To determine the tunnelling decay rates of conformer ***ttc*/VIp**, the intensity change of its three intensive transitions, the bands corresponding the O(H/D) and the C═O stretching and the C−O−(H/D) bending fundamentals, was analyzed. The half-lives obtained from the decay of these three bands gave the same result within the experimental uncertainty. (Since the intensity change of ***ttt*/Ip** is also influenced by the ***ttt*/Ip** ↔ ***tct*/IIIp** conversion process, it cannot be used directly for the accurate determination of the ***ttc*/VIp** → ***ttt*/Ip** tunneling rate.) Figures 7 and 8 show the measured relative intensity of the bands of glycine and glycine-d_3 in Ar, Kr, and Xe matrices as the function of time together with single exponential curves fitted to the decay. These fits resulted in half-lives of 4.4 ± 1 s, 4.0 ± 1 s, and 2.8 ± 1 s for glycine ***ttc*/VIp**, and 53.7 ± 1 h, 48.0 ± 1 h, and 99.3 ± 2 h for glycine-d_3 ***ttc*/VIp** in Ar, Kr, and Xe matrices, respectively.

The measured half-life of the ***ttc*/VIp** conformer of glycine and the computed ***ttc*/VIp** → ***ttt*/Ip** barrier height are consistent with earlier results obtained for the *cis* forms of simpler carboxylic acids,[9,38] showing a correlation between the experimental half-lives and computed barrier heights. In detail, the experimental half-lives for glycine, propionic, acetic, formic, and 2-chloropropionic acid in Ar at 12−15 K are 5, 14, 35, 350, and ∼2 × 10^5 s, while the MP2/6-311++G** barrier heights are 2147, 2290, 2308, 2676, and 2849 cm^{-1}, respectively. In the case of chloroacetic acid, for which the MP2/6-311++G** *cis* → *trans* barrier height is 3122 cm^{-1},[38] no tunneling was observed on the experimental time scale.[97] The roughly 2 day-long half-life of glycine-d_3 is also consistent with the ∼10 days half-life (∼15 days lifetime) of *cis*-CH_3COOD and *cis*-HCOOD in an 8 K Ar matrix.[12,17]

Although the simple one-dimensional Eckart model predicts a relatively fast tunneling process, it overestimates the experimental observations. Using the MP2/6-311++G** barrier height, the relative energies of the ***ttt*/Ip** and ***ttc*/VIp** conformers, and the unscaled MP2/6-311++G** harmonic frequencies, 658 and 383 s were computed for the half-life of glycine at 12 and 15 K, respectively. The computed ***ttc*/VIp** to ***ttt*/Ip** classical conversion rate over this barrier is practically zero at both 12 and 15 K; 2 × 10^{100} and 6 × 10^{77} s half-lives were obtained, respectively.

According to expectations, a more polarizable medium stabilizes the *cis* conformer compared to the *cis*−*trans* transition structure of carboxylic acids, and therefore the tunneling rates should decrease.[5,12] However, the experimentally measured tunneling rates of "*cis*-type" ***ttc*/VIp** conformer of glycine are almost equal and have a reverse order ($k_{Xe} \geq k_{Kr} \approx k_{Ar}$) in different noble gas matrices. The tunneling rates of glycine-d_3 ***ttc*/VIp** in Kr and Ar are also the same within experimental accuracy ($k_{Xe} \geq k_{Ar} \approx k_{Kr}$). Similar "anomalous" behavior was observed for *cis*-HCOOD[12] and *cis*-acetic acid,[17] which can be interpreted by different couplings of "*cis*" and "*trans*" vibrational states and the different rate of energy dissipation in the different matrices.[5,12]

Fitting a single exponential decay curve on the observed intensity decrease of glycine ***ttc*/VIp** bands in N_2 matrix at 12 K resulted in half-lives of 6.69 × 10^3 and 1.38 × 10^4 s for glycine ***ttc*/VIp** in sites A and B, respectively (see Figure 9). Note that the decay curve fitted for the faster decaying A site slightly deviates from the experimental data. This can be explained by the IR bands assigned to this site corresponding to two or more subsites unresolved in the spectra, but having a slightly different lifetime for glycine ***ttc*/VIp**. This proposition is supported by

dx.doi.org/10.1021/jp3076436 | J. Phys. Chem. A 2012, 116, 10539−10547

Table 3. Computed (SQM B3LYP) Fundamental Frequencies ($\tilde{\nu}$ in cm^{-1}), Intensities (I in km mol^{-1}) and Experimental Vibrational Transitions ($\tilde{\nu}$ in cm^{-1}) of the *ttc*/VIp Conformer of Glycine-d_3

$\tilde{\nu}$	I	Ar matrix	Kr matrix	Xe matrix	N_2 matrix
2937	11	2950.6w			2941.9w
2900	28	2927.7w	2922.0w		2917.0w
2624	27	2658.7s, 2661.6w, 2666.7w	2655.7s	2645.8s, 2640.0w	2651.7s, 2655.9w, 2645.0w
2524	6				
2422	3				
1788	271	1804.3vs	1802.4s, 1798.9m	1795.5vs	1802.4m, 1799.5s, 1791.9s, 1787.6m
1434	7				
1357	9	1343.7w		1340.0w	
1290	0				
1216	53				
1185	283	1196.3vs, 1193.4s	1198.2vs, 1194.5w	1199.3s, 1197.8sh	1210.7vs, 1205.4m
1064	54	1084.8w	1081.7w	1080.5w	
1058	1				
918	2				
806	52	827.3m	827.5m	826.8m	823.1m
779	2				
718	59	715.5m	712.9w	715.7m	720.4m
603	24	604.4w		604.2w	
533	0				
425	2				
335	57				
241	30				
169	38				
64	7				

the observation that the shape of the C−O−H bending fundamental band corresponding to this site changes during the decay; the lower wavenumber side decays slightly faster than its higher wavenumber side. The half-life of glycine-d_3 ***ttc*/VIp** in the N_2 matrix is extremely large. It cannot be determined experimentally, and it is estimated to be on the time scale of weeks.

Figure 10 shows the temperature dependence of the tunnelling rates of glycine ***ttc*/VIp** in a N_2 matrix. These curves are qualitatively similar to the ones observed for formic and acetic acid in a N_2 matrix.[13,14] The slow increase with temperature clearly shows that the decay rate is determined solely by the tunnelling mechanism at low temperatures (<16−18 K). As it was mentioned above, the 3 orders of magnitude longer lifetime of conformer ***ttc*/VIp** in a N_2 matrix compared to Ar, Kr, and Xe matrices was expected based on former studies.[13,14] In the case of acetic and formic acid, the extended lifetime was explained by complex formation between the carboxylic OH and a N_2 molecule decreasing the energy of the *cis* form compared to that of the *trans* and the transition structure. A related, alternative explanation is that based on the quadrupole moment of N_2. In a nitrogen matrix, the *cis* form with larger dipole moment (μ_e(***ttc*/VIp**) = 3.2 D at the B3LYP/6-31++G** level of theory) is stabilized more compared to the transition structure and the *trans* form ((μ_e(**TS**) = 2.8 D, and μ_e(***ttt*/Ip**) = 1.2 D at the B3LYP/6-31++G** level of theory), which have smaller dipole moments.[13,14]

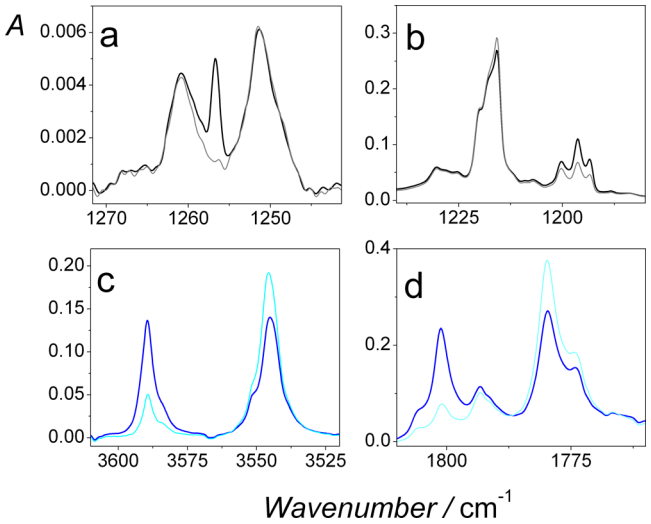

Figure 6. Spectral regions selected for the demonstration of the dark process. (a) C−O−H bending region of glycine in Ar matrix after NIR irradiation at 6946 cm^{-1} (thick black line) and after leaving in the dark for ∼30 s (thin gray line); (b) C−O−D bending region of glycine-d_3 in Ar matrix after NIR irradiation at 5167 cm^{-1} (thick black line) and after leaving in he dark for ∼2 days (thin gray line); (c,d) O−H and stretching C═O stretching regions of glycine in N_2 matrix (thick blue line) and after leaving in the dark for ∼2.5 h (thin light blue line). See the list of the decreasing bands of conformer ***ttc*/VIp** in Tables 2 and 3, and the increasing bands of conformer ***ttt*/Ip** in the Supporting Information.

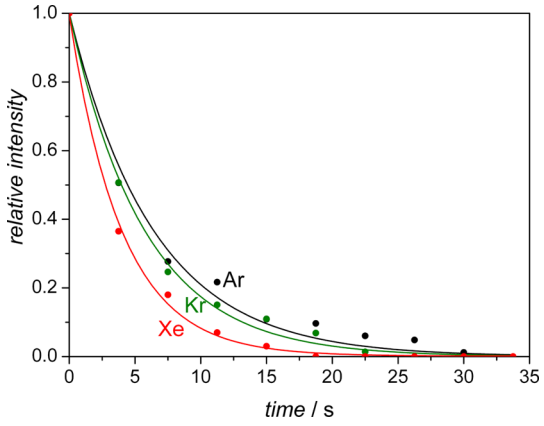

Figure 7. The decay of glycine conformer ***ttc*/VIp** in Ar (black), Kr (green), and Xe (red) matrices. (Symbols: experimental measurements; lines: fitted single exponential decays.).

In addition to the ***ttc*/VIp** → ***ttt*/Ip** conversion, especially if the amount of ***tct*/IIIp** was changed by the NIR irradiation, the ***tct*/IIIp** ↔ ***ttt*/Ip** conversion process was also observed in the dark. According to MP2/6-311++G** and B3LYP/6-31++G** computations, the barrier from glycine ***tct*/IIIp** to ***ttt*/Ip** along the C−C−O−H deformation coordinate is only 282 cm^{-1} and 335.2 cm^{-1}, respectively. This barrier can be crossed classically even at 12 K on the ∼1−10^4 s time scale.[98,99] In contrast to the faster ***ttc*/VIp** → ***ttt*/Ip** conversion, the ***tct*/IIIp** ↔ ***ttt*/Ip** process can be accelerated by the >3850 cm^{-1} radiation of the source of the spectrometer. Thus this conversion is not a tunneling process and its detailed analysis is beyond the scope of the present study.

dx.doi.org/10.1021/jp3076436 | J. Phys. Chem. A 2012, 116, 10539−10547

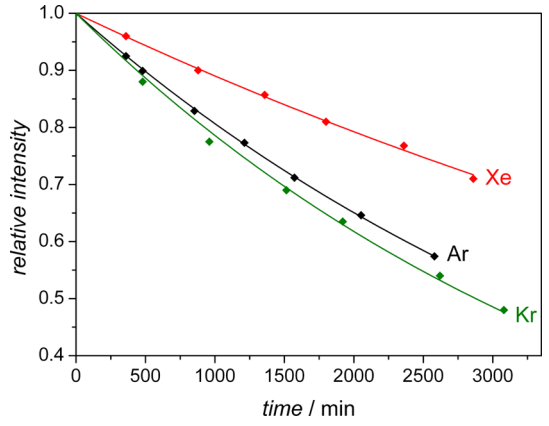

Figure 8. The decay of bands of glycine-d_3 conformer ***ttc*/VIp** in Ar (black), Kr (green), and Xe (red) matrices. (Symbols: experimental measurements; lines: fitted single exponential decays.).

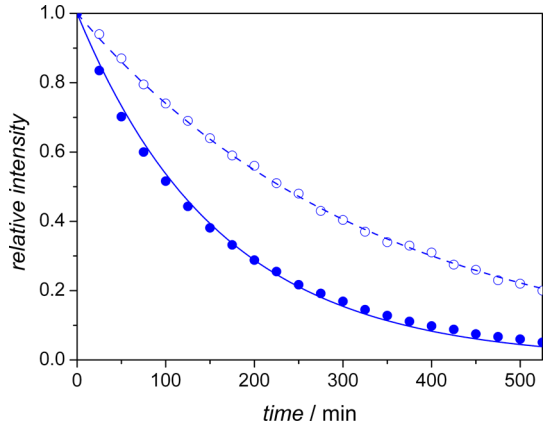

Figure 9. The decay of bands of glycine conformer ***ttc*/VIp** in the two different sites (site A: solid line and filled symbols; site B: dashed line and empty symbols) found in N_2 matrices. (Symbols: experimental measurements; lines: fitted single exponential decays.).

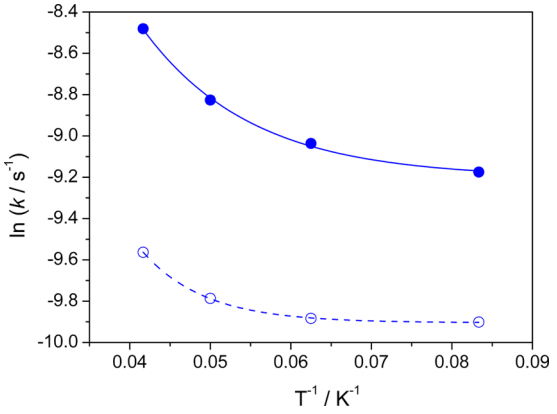

Figure 10. The temperature dependence of the tunneling rates of glycine conformer ***ttc*/VIp** in the two different sites (site A: solid line and filled symbols; site B: dashed line and empty symbols) of a N_2 matrix.

4. SUMMARY AND CONCLUSIONS

In the present paper, the IR spectrum and the tunneling decay rates of the short-lived ***ttc*/VIp** conformer of glycine and glycine-N,N,O-d_3 in Ar, Kr, Xe, and N_2 matrices have been reported. The 2.8−4.4 s half-life of glycine ***ttc*/VIp** in Ar, Kr, and Xe matrices at 12 K is shorter than that of simple carboxylic acids, including formic, acetic, propionic, and 2-chloropropionic acid.[9,38] Due to complex formation with the host molecules, the half-life of glycine ***ttc*/VIp** is more than 3 orders of magnitude longer in N_2 matrix. For glycine-N,N,O-d_3, the half-life is on the order of days in Ar, Kr, and Xe matrices, while it is estimated to be over weeks in N_2 matrix.

These results clearly support the hypothesis of Schreiner and co-workers,[100] who have suggested that specific conformers of amino acids can decay by fast tunneling under matrix-isolation conditions, making the observation of these species challenging. Besides conformers with a "*cis*-type" carboxylic group, like glycine ***ttc*/VIp**, the higher energy rotamers of the amino group and the rotamers of the hydroxyl groups in the side chain of serine, threonine, and tyrosine might also be depleted by tunneling. Fast tunneling might explain the lack of observations of the low-energy ***gtt*/IVn** conformer of glycine and of some conformers of other amino acids in low-temperature matrices.

The present and former[12,14] studies reveal that the tunneling decay of a higher energy conformer can be slowed down using N_2 as host instead of noble gas matrices, in addition to the H−D isotopic substitution. Although in our preliminary experiments, when the first overtone of the OH and NH stretchings and their combination bands of glycine ***ttt*/Ip** were irradiated in N_2 matrix we did not observe the formation of new conformers, a more systematic work to prepare the remaining unobserved conformers of glycine and measure their tunneling rate is in progress.

■ ASSOCIATED CONTENT

Ⓢ Supporting Information

Assignments of MI-IR spectra of ***ttt*/Ip**, ***ccc*/IIn**, and ***tct*/IIIp** conformers of glycine and glycine-d_3 in Ar, Kr, Xe, and N_2 matrices. This material is available free of charge via the Internet at http://pubs.acs.org.

■ AUTHOR INFORMATION

Notes

The authors declare no competing financial interest.

■ ACKNOWLEDGMENTS

This work was funded by the Hungarian Scientific Research Fund (OTKA K75877). The European Union and the European Social Fund have provided financial support to the project under Grant No. TAMOP 4.2.1./B-09/KMR-2010-0003. G.T. gratefully acknowledges Prof. György Michaletzky (Dean of Faculty of Sciences, Eötvös University) and Prof. Péter Surján (Head of Institute of Chemistry, Eötvös University) for their support of establishing the laser spectroscopy facility at Eötvös University.

■ REFERENCES

(1) Aspiala, A.; Lotta, T.; Murto, J.; Räsänen, M. *J. Chem. Phys.* **1983**, *79*, 4183−4192.
(2) Kudoh, S.; Takayanagi, M.; Nakata, M.; Ishibashi, T.; Tasumi, M. *J. Mol. Struct.* **1999**, *479*, 41−52.
(3) Pettersson, M.; Lundell, J.; Khriachtchev, L.; Räsänen, M. *J. Am. Chem. Soc.* **1997**, *119*, 11715−11716.
(4) Khriachtchev, L.; Maçôas, E.; Pettersson, M.; Räsänen, M. *J. Am. Chem. Soc.* **2002**, *124*, 10994−10995.
(5) Pettersson, M.; Maçôas, E. M. S.; Khriachtchev, L.; Lundell, J.; Fausto, R.; Räsänen, M. *J. Chem. Phys.* **2002**, *117*, 9095−9098.

(6) Maçôas, E. M. S.; Khriachtchev, L.; Pettersson, M.; Juselius, J.; Fausto, R.; Räsänen, M. *J. Chem. Phys.* **2003**, *119*, 11765−11772.
(7) Pettersson, M.; Maçôas, E. M. S.; Khriachtchev, L.; Fausto, R.; Räsänen, M. *J. Am. Chem. Soc.* **2003**, *125*, 4058−4059.
(8) Maçôas, E. M. S.; Khriachtchev, L.; Pettersson, M.; Lundell, J.; Fausto, R.; Räsänen, M. *Vib. Spectrosc.* **2004**, *34*, 73−82.
(9) Maçôas, E. M. S.; Khriachtchev, L.; Pettersson, M.; Fausto, R.; Räsänen, M. *Phys. Chem. Chem. Phys.* **2005**, *7*, 743−749.
(10) Marushkevich, K.; Khriachtchev, L.; Räsänen, M. *J. Chem. Phys.* **2007**, *126*, 241102−1−4.
(11) Marushkevich, K.; Khriachtchev, L.; Räsänen, M. *Phys. Chem. Chem. Phys.* **2007**, *9*, 5748−5751.
(12) Domanskaya, A. V.; Marushkevich, K.; Räsänen, M.; Khriachtchev, L. *J. Chem. Phys.* **2009**, *130*, 154509-1−5.
(13) Marushkevich, K.; Räsänen, M.; Khriachtchev, L. *J. Phys. Chem. A* **2010**, *114*, 10584−10589.
(14) Lopes, S.; Domanskaya, A. V.; Fausto, R.; Räsänen, M.; Khriachtchev, L. *J. Chem. Phys.* **2010**, *133*, 144507-1−7.
(15) Maçôas, E. M. S.; Khriachtchev, L.; Pettersson, M.; Fausto, R.; Räsänen, M. *J. Am. Chem. Soc.* **2003**, *125*, 16188−16189.
(16) Maçôas, E. M. S.; Khriachtchev, L.; Fausto, R.; Räsänen, M. *J. Phys. Chem. A* **2004**, *108*, 3380−3389.
(17) Maçôas, E. M. S.; Khriachtchev, L.; Pettersson, M.; Fausto, R.; Räsänen, M. *J. Chem. Phys.* **2004**, *121*, 1331−1338.
(18) Maçôas, E. M. S.; Khriachtchev, L.; Pettersson, M.; Fausto, R.; Räsänen, M. *J. Phys. Chem. A* **2005**, *109*, 3617−3625.
(19) Isoniemi, E.; Khriachtchev, L.; Makkonen, M.; Räsänen, M. *J. Phys. Chem. A* **2006**, *110*, 11479−11487.
(20) Tsuge, M.; Marushkevich, K.; Räsänen, M.; Khriachtchev, L. *J. Phys. Chem. A* **2012**, *116*, 5305−5311.
(21) Akai, N.; Kudoh, S.; Takayanagi, M.; Nakata, M. *Chem. Phys. Lett.* **2002**, *356*, 133−139.
(22) Akai, N.; Kudoh, S.; Nakata, M. *J. Phys. Chem. A* **2003**, *107*, 3655−3659.
(23) Akai, N.; Kudoh, S.; Nakata, M. *J. Photochem. Photobiol., A* **2005**, *169*, 47−55.
(24) Ichimura, K.; Futami, Y.; Kudoh, S.; Nakata, M. *Chem. Phys. Lett.* **2004**, *391*, 50−55.
(25) Nagaya, M.; Nakata, M. *J. Phys. Chem. A* **2007**, *111*, 6256−6262.
(26) Nishino, S.; Nakata, M. *J. Phys. Chem. A* **2007**, *111*, 7041−7047.
(27) Amiri, S.; Reisenauer, H. P.; Schreiner, P. R. *J. Am. Chem. Soc.* **2010**, *132*, 15902−15904.
(28) Walla, P. J.; Nickel, B. *Chem. Phys.* **2005**, *312*, 177−185.
(29) Rostkowska, H.; Lapinski, L.; Khvorostov, A.; Nowak, M. J. *J. Phys. Chem. A* **2003**, *107*, 6373−6380.
(30) Rostkowska, H.; Lapinski, L.; Khvorostov, A.; Nowak, M. J. *Chem. Phys.* **2004**, *298*, 223−232.
(31) Lapinski, L.; Rostkowska, H.; Khvorostov, A.; Yaman, M.; Fausto, R.; Nowak, M. J. *J. Phys. Chem. A* **2004**, *108*, 5551−5558.
(32) Nakane, N.; Enyo, T.; Tomioka, H. *J. Org. Chem.* **2004**, *69*, 3538−3545.
(33) Schreiner, P. R.; Reisenauer, H. P.; Pickard, F. C.; Simmonett, A. C.; Allen, W. D.; Mátyus, E.; Császár, A. G. *Nature* **2008**, *453*, 906−909.
(34) Gerbig, D.; Reisenauer, H. P.; Wu, C. H.; Ley, D.; Allen, W. D.; Schreiner, P. R. *J. Am. Chem. Soc.* **2010**, *132*, 7273−7275.
(35) Schreiner, P. R.; Reisenauer, H. P.; Ley, D.; Gerbig, D.; Wu, C. H.; Allen, W. D. *Science* **2011**, *332*, 1300−1303.
(36) Gerbig, D.; Ley, D.; Schreiner, P. R. *Org. Lett.* **2011**, *13*, 3526−3529.
(37) Bednarek, P.; Zhu, Z.; Bally, T.; Filipiak, T.; Marcinek, A.; Gebicki, J. *J. Am. Chem. Soc.* **2001**, *123*, 2377−2387.
(38) Bazsó, G.; Góbi, S.; Tarczay, G. *J. Phys. Chem. A* **2012**, *116*, 4823−4832.
(39) Cao, Q.; Melavuori, M.; Lundell, J.; Räsänen, M.; Khriachtchev, L. *J. Mol. Struct.* **2012**, DOI: 10.1016/j.molstruc.2012.05.027.
(40) Reva, I.; Nowak, M. J.; Lapinski, L.; Fausto, R. *J. Chem. Phys.* **2012**, *136*, 064511−1−8.
(41) Marcinek, A.; Adamus, J.; Huzben, K.; Gebicki, J.; Bartczak, T. J.; Bednarek, P.; Bally, T. *J. Am. Chem. Soc.* **2000**, *122*, 437.
(42) Bazsó, G.; Magyarfalvi, G.; Tarczay, G. *J. Mol. Struct.* **2012**, DOI: 10.1016/j.molstruc.2012.04.066.
(43) Cha, Y.; Murray, C. J.; Klinman, J. P. *Science* **1989**, *243*, 1325−1330.
(44) Kohen, A.; Klinman, J. P. *Chem. Biol.* **1999**, *6*, R191−198.
(45) Brown, R. D.; Godfrey, P. D.; Storey, J. W. V.; Bassez, M. P. *J. Chem. Soc., Chem. Commun.* **1978**, 547−548.
(46) Suenram, R. D.; Lovas, F. J. *J. Mol. Spectrosc.* **1978**, *72*, 372−382.
(47) Sellers, H. L.; Schäfer, L. *J. Am. Chem. Soc.* **1978**, *100*, 7728−7729.
(48) Schäfer, L.; Sellers, H. L.; Lovas, F. J.; Suernam, R. D. *J. Am. Chem. Soc.* **1980**, *102*, 6566−6568.
(49) Suenram, R. D.; Lovas, F. J. *J. Am. Chem. Soc.* **1980**, *102*, 7180−7184.
(50) Lovas, F. J.; Kawashima, Y.; Grabow, J.-U.; Suenram, R. D.; Freser, G. T.; Hirota, E. *Astrophys. J.* **1995**, *455*, L201−L204.
(51) Godfrey, P. D.; Brown, R. D. *J. Am. Chem. Soc.* **1995**, *117*, 2019−2023.
(52) McGlone, S. J.; Elmes, P. S.; Brown, R. D.; Godfrey, P. D. *J. Mol. Struct.* **1999**, *485−486*, 225−238.
(53) Grenie, Y.; Lassegues, J. C.; Garrigou-Lagrange, C. *J. Chem. Phys.* **1970**, *53*, 2980−2982.
(54) Grenie, Y.; Garrigou-Lagrange, C. *J. Mol. Spectrosc.* **1972**, *41*, 240−248.
(55) Reva, I. D.; Plokhotnichenko, A. M.; Stepanian, S. G.; Ivanov, A. Yu.; Radchenko, E. D.; Sheina, G. G.; Blagoi, Yu. P. *Chem. Phys. Lett.* **1995**, *232*, 141−148; Erratum. *Chem. Phys. Lett.* **1995**, *235*, 617.
(56) Stepanian, S. G.; Reva, I. D.; Radchenko, E. D.; Rosado, M. T. S.; Duarte, M. L. T. S.; Fausto, R.; Adamowicz, L. *J. Phys. Chem. A* **1998**, *102*, 1041−1054.
(57) Ivanov, A. Yu.; Plokhotnichenko, A. M.; Izvekov, V.; Sheina, G. G.; Blagoi, Yu. P. *J. Mol. Struct.* **1997**, *408−409*, 459−462.
(58) Ivanov, A. Yu.; Sheina, G.; Blagoi, Yu. P. *Spectrochim. Acta, Part A* **1999**, *55*, 219−228.
(59) Huisken, F.; Werhahn, O.; Ivanov, A. Yu.; Krasnokutski, S. A. *J. Chem. Phys.* **1999**, *111*, 2978−2984.
(60) Ramaekers, R.; Pajak, J.; Lambie, B.; Maes, G. *J. Chem. Phys.* **2004**, *120*, 4182−4193.
(61) Espinoza, C.; Szczepanski, J.; Vala, M.; Polfer, N. C. *J. Phys. Chem. A* **2010**, *114*, 5919−5927.
(62) Balabin, R. M. *J. Phys. Chem. Lett.* **2010**, *1*, 20−23.
(63) Vishveshwara, S.; Pople, J. A. *J. Am. Chem. Soc.* **1977**, *99*, 2422−2426.
(64) Ramek, M.; Cheng, V. K. W.; Frey, R. F.; Newton, S. Q.; Schäfer, L. *J. Mol. Struct. (THEOCHEM)* **1991**, *235*, 1−10.
(65) Jensen, J. H.; Gordon, M. S. *J. Am. Chem. Soc.* **1991**, *113*, 7917−7924.
(66) Yu, D.; Armstrong, D. A.; Rauk, A. *Can. J. Chem.* **1992**, *70*, 1762−1772.
(67) Frey, R. F.; Coffin, J.; Newton, S. Q.; Ramek, M.; Cheng, V. K. W.; Momany, F. A.; Schäfer, L. *J. Am. Chem. Soc.* **1992**, *114*, 5369−5377.
(68) Császár, A. *J. Am. Chem. Soc.* **1992**, *114*, 9568−9575.
(69) Hu, C. H.; Shen, M.; Schaefer, H. F. *J. Am. Chem. Soc.* **1993**, *115*, 2923−2929.
(70) Lelj, F.; Adamo, C.; Barone, V. *Chem. Phys. Lett.* **1994**, *230*, 189−195.
(71) Hoyau, S.; Ohanessian, G. *J. Am. Chem. Soc.* **1997**, *119*, 2016−2024.
(72) Barone, V.; Adamo, C.; Lelj, F. *J. Chem. Phys.* **1995**, *102*, 364−368.
(73) Yu, D.; Rauk, A.; Armstrong, D. A. *J. Am. Chem. Soc.* **1995**, *117*, 1789−1796.
(74) Császár, A. *J. Mol. Struct.* **1995**, *346*, 141−152.
(75) Kieninger, M.; Suhai, S.; Ventura, O. N. *J. Mol. Struct. (THEOCHEM)* **1998**, *433*, 193−201.

(76) Pacios, L. F.; Galvez, O.; Gomez, P. C. *J. Phys. Chem. A* **2001**, *105*, 5232−5241.
(77) Bludský, O.; Chocholoušová, J.; Vacek, J.; Huisken, F.; Hobza, P. *J. Chem. Phys.* **2000**, *113*, 4629−4635.
(78) Miller, T. F., III; Clary, D. C. *Phys. Chem. Chem. Phys.* **2004**, *6*, 2563−2571.
(79) Ke, H.-W.; Rao, L.; Xu, X.; Yan, Y.-J. *J. Theor. Comput. Chem.* **2008**, *7*, 889−909.
(80) Balabin, R. M. *Chem. Phys. Lett.* **2009**, *479*, 195−200.
(81) Cormanich, R. A.; Ducati, L. C.; Rittner, R. *Chem. Phys.* **2011**, *387*, 85−91.
(82) Kayi, H.; Kaiser, R. I.; Head, J. D. *Phys. Chem. Chem. Phys.* **2011**, *13*, 15774−15784.
(83) Lattelais, M.; Pauzat, F.; Pilmé, J.; Ellinger, Y.; Ceccarelli, C. *Astron. Astrophys.* **2011**, *532*, A39.
(84) Godfrey, P. D.; Brown, R. D.; Rodgers, F. M. *J. Mol. Struct.* **1996**, *376*, 65−81.
(85) Miller, T. F., III; Clary, D. C.; Meijer, A. J. H. M. *J. Chem. Phys.* **2005**, *122*, 244323.
(86) (a) *PQS Version 3.2*; Parallel Quantum Solutions: Fayetteville, AR, 2006. (b) Baker, J.; Wolinski, K.; Malagoli, M.; Kinghorn, D.; Wolinski, P.; Magyarfalvi, G.; Saebo, S.; Janowski, T.; Pulay, P. *J. Comput. Chem.* **2009**, *30*, 317−335.
(87) Frisch, M. J.; Trucks, G. W.; Schlegel, H. B.; Scuseria, G. E.; Robb, M. A.; Cheeseman, J. R.; Scalmani, G.; Barone, V.; Mennucci, B.; Petersson, G. A. et al. *Gaussian 09*, revision A.1; Gaussian, Inc.: Wallingford, CT, 2009.
(88) (a) Becke, A. D. *J. Chem. Phys.* **1993**, *98*, 5648−5652. (b) Lee, C.; Yang, W.; Parr, R. G. *Phys. Rev. B* **1998**, *37*, 785−789.
(89) (a) Hehre, W. J.; Ditchfield, R.; Pople, J. A. *J. Chem. Phys.* **1972**, *56*, 2257−2261. (b) Francl, M. M.; Petro, W. J.; Hehre, W. J.; Binkley, J. S.; Gordon, M. S.; DeFrees, D. J.; Pople, J. A. *J. Chem. Phys.* **1982**, *77*, 3654−3665. (c) Clark, T.; Chandrasekhar, J.; Spitznagel, G. W.; Schleyer, P. v. R. *J. Comput. Chem.* **1983**, *4*, 294−301. (d) Krishnam, R.; Binkley, J. S.; Seeger, R.; Pople, J. A. *J. Chem. Phys.* **1980**, *72*, 650−654. (e) Gill, P. M. W.; Johnson, B. G.; Pople, J. A.; Frisch, M. J. *Chem. Phys. Lett.* **1992**, *197*, 499−505.
(90) Møller, C.; Plesset, M. S. *Phys. Rev.* **1934**, *46*, 618−622.
(91) (a) Hehre, W. J.; Ditchfield, R.; Pople, J. A. *J. Chem. Phys.* **1972**, *56*, 2257−2261. (b) Francl, M. M.; Petro, W. J.; Hehre, W. J.; Binkley, J. S.; Gordon, M. S.; DeFrees, D. J.; Pople, J. A. *J. Chem. Phys.* **1982**, *77*, 3654−3665. (c) Clark, T.; Chandrasekhar, J.; Spitznagel, G. W.; Schleyer, P. v. R. *J. Comput. Chem.* **1983**, *4*, 294−301. (d) Krishnam, R.; Binkley, J. S.; Seeger, R.; Pople, J. A. *J. Chem. Phys.* **1980**, *72*, 650−654. (e) Gill, P. M. W.; Johnson, B. G.; Pople, J. A.; Frisch, M. J. *Chem. Phys. Lett.* **1992**, *197*, 499−505.
(92) Pulay, P.; Fogarasi, G.; Pongor, G.; Boggs, J. E.; Vargha, A. *J. Am. Chem. Soc.* **1983**, *105*, 7037−7047.
(93) Baker, J.; Jarzecki, A. A.; Pulay, P. *J. Phys. Chem. A* **1998**, *102*, 1412−1424.
(94) Fábri, C.; Szidarovszky, T.; Magyarfalvi, G.; Tarczay, G. *J. Phys. Chem. A* **2011**, *115*, 4640−4649.
(95) (a) *MultiWell-2011.1 Software*, designed and maintained by Barker, J. R. with contributors Ortiz, N. F.; Preses, J. M.; Lohr, L. L.; Maranzana, A.; Stimac, P. J.; Nguyen, T. L., Dhilip Kumar, T. J.; University of Michigan: Ann Arbor, MI, 2011; http://aoss.engin.umich.edu/multiwell/. (b) Barker, J. R. *Int. J. Chem. Kinetics* **2011**, *33*, 232−245. (c) Barker, J. R. *Int. J. Chem. Kinetics* **2009**, *41*, 748−763.
(96) Eckart, C. *Phys. Rev.* **1930**, *35*, 1303−1309.
(97) Nieminen, J.; Pettersson, M.; Räsänen, M. *J. Chem. Phys.* **1993**, *97*, 10925−10936.
(98) Barnes, A. J. *J. Mol. Struct.* **1984**, *113*, 161−174.
(99) Our simulation by Multiwell predicted a 1.9 s half-life for gas phase at 12 K. The measured values for the glycine and its deuterated isotopologue in different matrices are on the time scale of seconds to hours.
(100) Schreiner, P. R., Justus-Liebig-University of Giessen, Germany, Allen, W. D.Center for Computational Quantum Chemistry, The University of Georgia, Athens, Georgia, USA; Private communication.